The role of rejuvenators in embedded damage healing for asphalt pavement

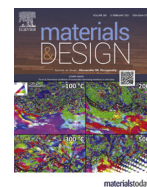Xu, S.; Liu, X.; Tabaković, A.; Lin, P.; Zhang, Y.; Nahar, S.; Lommerts, B. J.; Schlangen, E.

Important note
To cite this publication, please use the final published version (if applicable).
Please check the document version above.

The role of rejuvenators in embedded damage healing for asphalt pavement

S. Xu [a,*], X. Liu [a], A. Tabaković [a,b,c], P. Lin [a,d], Y. Zhang [a,e], S. Nahar [f,g], B.J. Lommerts [f,h], E. Schlangen [a]

[a] Civil Engineering and Geosciences, Delft University of Technology, Delft 2628CN, the Netherlands
[b] Centre for Research in Engineering Surface Technology (CREST), Technological University Dublin, D08 CKP1, Ireland
[c] School of Civil Engineering, University College Dublin, Dublin D04 K3H4, Ireland
[d] Key Laboratory of Road and Traffic Engineering of the Ministry of Education, Tongji University, Shanghai 200092, China
[e] School of Highway, Chang'an University, Xi'an 710064, Shaanxi, China
[f] Latexfalt B.V., Koudekerk aan den Rijn 2396 AP, the Netherlands
[g] TNO Science and Industry, Delft 2628 CK, the Netherlands
[h] Xiyuefa Group, Taiyuan 030006, Shanxi, China

HIGHLIGHTS

- The rejuvenator dosage used in the capsule healing system is less than that in RAP.
- The type and amount of rejuvenator need to be optimized for the capsule healing system.
- Re-ageing test is important in the evaluation of a rejuvenator.
- The calcium alginate capsules are capable of encapsulating different rejuvenators.
- The encapsulated rejuvenator largely determines the capsule performance.

GRAPHICAL ABSTRACT
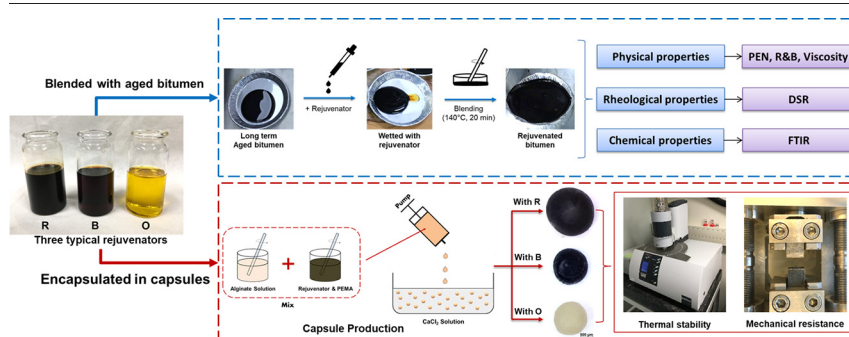
ABSTRACT

Rejuvenator encapsulation technique showed great potential for extrinsic asphalt pavement damage healing. Once the capsules are embedded within asphalt pavement, the healing is activated on-demand via progressing microcrack. When the microcrack encounters the capsule, the fracture energy at the tip opens the capsule and releases the rejuvenator. Then the released rejuvenator wets the crack surfaces, diffuses into and softens the aged bitumen, allowing two broken edges to come in the contact, preventing further asphalt pavement deterioration. The quality and speed of the damage repair process strongly depend on the quality of rejuvenator, thus it is important to choose a proper rejuvenator with good abilities to restore the lost properties of bitumen from ageing and show a sustainable performance after healing. To this aim, three different rejuvenators were studied and ranked based on the performance of their rejuvenated bitumen, including physical properties, rheological properties, chemical properties and the performance after re-ageing. Furthermore, these rejuvenators were encapsulated in calcium alginate capsules and the tests on these capsules indicate the diameter, mechanical resistance and thermal stability of the capsules are influenced by the encapsulated rejuvenator. The findings will benefit the development of rejuvenator encapsulation technique and the optimization of the capsule healing system towards a better healing effect in asphalt pavement.

---

* Corresponding author.
  E-mail address: s.xu-1@tudelft.nl (S. Xu).

1. Introduction

Asphalt pavement is a heterogeneous material composed of coarse aggregates, sand, filler and bitumen. Bitumen is a material within the mix that binds the asphalt pavement mix, gives it flexibility and ability to heal. However, overtime bitumen ageing takes place due to environmental conditions (Oxygen, UV light, moisture, etc), causing it to lose its volatile chemical compounds, making it brittle and prone to cracking which in turn can cause premature asphalt pavement failure [1–5].

However, the effects of bitumen ageing can be reversed. The bitumen rejuvenator can be used to reverse the effects of bitumen ageing process by restoring the lost properties, i.e., chemical composition, physical properties and rheological properties [6–8].

The bitumen rejuvenation highly depends on the rejuvenator type and dosage [9]. Bitumen with a high penetration level (70/100 or higher) is often used in industry to soften the aged bitumen. General rejuvenator types include bio-based rejuvenators either pure or stemming from waste streams, chemically modified rejuvenators and maltene rich fractions produced in oil refining processes and the recommended dosage ranges from 2% to 20% (by weight of bitumen) which is highly dependent on the rejuvenator type and the characteristics of the aged bitumen (e.g., ageing level) [9–13].

The bitumen rejuvenator can be applied in three ways: i) rejuvenation of reclaimed asphalt pavement (RAP), ii) asphalt pavement surface treatment (e.g., fog sealing), and iii) embedded rejuvenator encapsulation (e.g., capsules and fibres) [14]. For different rejuvenation purposes, the rejuvenator usage and dosage vary in these applications:

i. In the production of RAP, a rejuvenation process on old aggregates is always needed before mixing with the fresh material. For such reason, the rejuvenator is usually used to form a low viscosity layer and rejuvenate the aged bitumen of the reclaimed asphalt, and by this means, the recycled asphalt can be reused as part of a new asphalt pavement [15–17]. The type and amount of rejuvenator need to be properly determined to optimize the performance of pavement with RAP [14,18]. Although the use of RAP successfully achieves the recycling of aged asphalt, the recycling process involves removal, milling, and crushing of the old pavement, which consumes plenty of resources and energy and may result in a huge delay of traffic [14].

ii. When an asphalt pavement shows early signs of distress after around 3 to 7 years of service, a fog seal treatment can be employed on the surface layer, thus prevent or delay the damaging process and finally extend the pavement lifespan. The fog seal treatment not only rejuvenates the aged bitumen in the top portion of the surface layer but also seals cracks against intrusion of air and water to prevent serious damages like ravelling [14,19]. However, the sprayed rejuvenator can penetrate only 5 to 10 mm of a dense surface layer and no more than 20 mm of a porous surface layer, which means the majority depth of asphalt layer cannot be covered. Besides, it is also reported that some of the fog seal treatment can

reduce the skid resistance of an asphalt pavement [20]. To enhance the internal coating of porous asphalt an air jet is sometimes applied to force the rejuvenator into the open-graded pavement.

iii. The rejuvenator can also be encapsulated and embedded in an asphalt pavement (i.e. capsule healing system), thus rejuvenate the aged bitumen when the rejuvenator is released upon damaging, and finally, heal the damage. For this purpose, different rejuvenator encapsulating techniques have been proposed, such as calcium alginate capsules [21–24], alginate fibres [25,26], Malamine-Formaldehyde microcapsules [27], epoxy capsules [28], polyurethane/urea-formaldehyde microcapsules [29], etc. Fig. 1 shows that, with target asphalt binder at different ageing levels, the amount of rejuvenator needed for the capsule healing system is much lower than the amount needed for the rejuvenation of RAP. RAP usually requires the rejuvenated bitumen to behave like the virgin bitumen to mix with new materials [19]. However, the rejuvenation from the capsule healing system works earlier and mainly focuses on accelerating the in-situ crack healing process in asphalt pavement, therefore the rejuvenated bitumen does not need to meet the condition of re-mixing.

In a capsule healing system, it is important to optimize the type and amount of the embedded rejuvenator, since insufficient rejuvenator release will result in inadequate healing and too much of released rejuvenator may cause asphalt failures, such as stripping and rutting [9,30]. The rejuvenator type plays an important role in the encapsulation process which may affect the performance of the capsule products.

As such, this study investigates the effects of various types and dosages of rejuvenator on the physical, rheological and chemical properties of aged bitumen, and evaluates the performance of the calcium alginate capsules encapsulating these rejuvenators for the application in self-healing asphalt. Fig. 2 presents the methodology used in the study of different rejuvenators, and the abbreviations in Fig. 2 are defined in Table 1. First, laboratory ageing methods including the Rolling Thin-Film Oven (RTFO) and Pressure Ageing Vessel (PAV) were employed to prepare bitumen samples with different ageing levels namely origin bitumen (virgin), short-term aged bitumen (after RTFO) and long-term aged bitumen (after RTFO + PAV). Afterwards, the long-term aged bitumen was blended with different rejuvenators, and the performance of rejuvenated bitumen was evaluated. To examine the stability of the rejuvenated bitumen [31], the properties of the rejuvenated bitumen after a re-ageing process were investigated. In this way, the rejuvenation effect of three different types of rejuvenator was studied and ranked, and the recommended type and amount of rejuvenator for the design of a capsule healing system was determined. Moreover, the prospects of these rejuvenators being encapsulated in calcium alginate capsules and the influence of encapsulated rejuvenators on diameter, mechanical resistance, and thermal stability of the capsules were investigated.
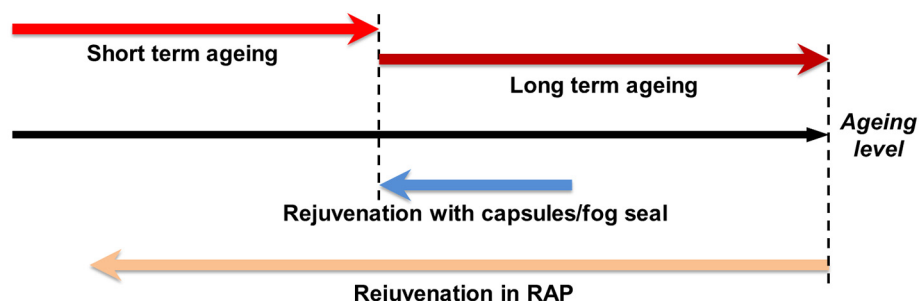

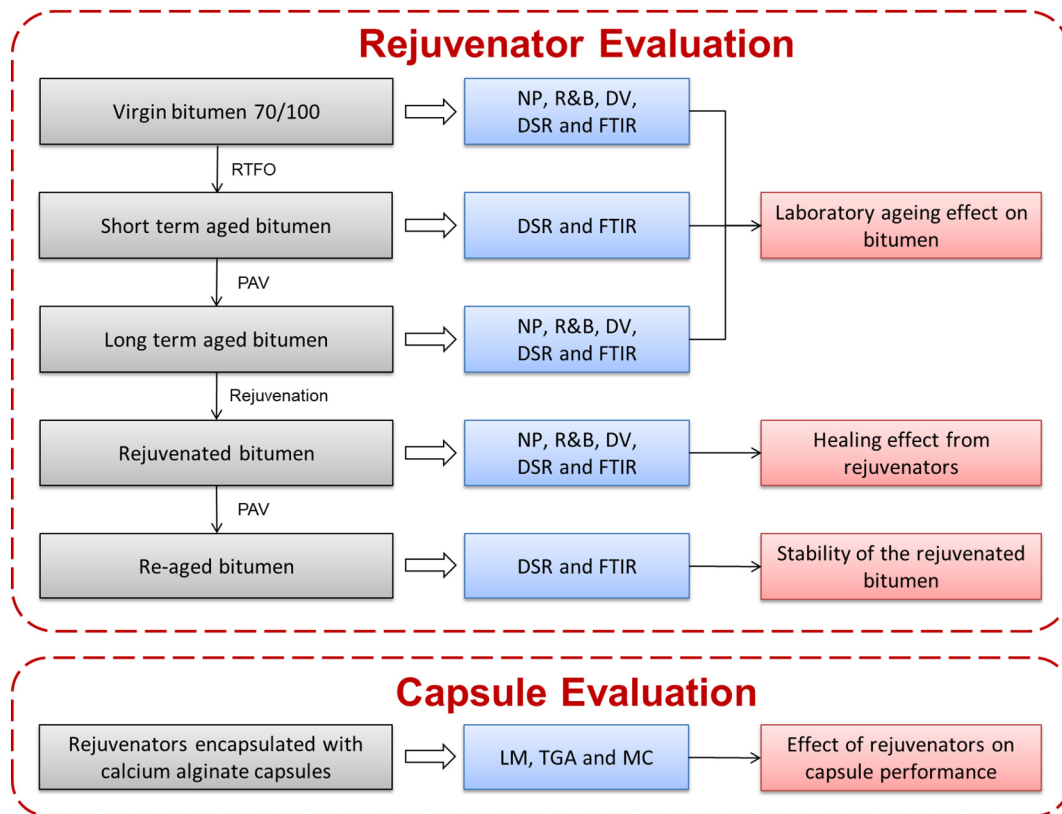**Fig. 1.** The rejuvenation needed in encapsulated rejuvenator and RAP.

Fig. 2. Methodology for rejuvenator study.

Table 1
List of abbreviations.

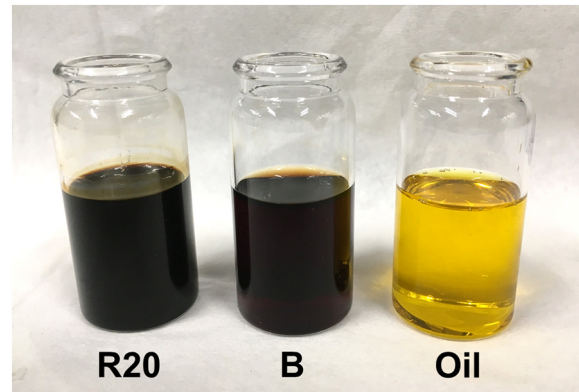| Abbreviations	Full name
RTFO	Rolling Thin-Film Oven
PAV	Pressure Ageing Vessel
NP	Needle Penetration
R&B	Ring and Ball
DV	Dynamic Viscosity
DSR	Dynamic Shear Rheometer
FTIR	Fourier-transform Infrared Spectroscopy
LM	Light Microscopy
TGA	Thermogravimetric Analysis
MC	Micro-compressive

Fig. 3. Image of three different rejuvenators.

2. Materials and methods

2.1. Bitumen and rejuvenators

The bitumen used in this study is the PEN 70/100 bitumen, which is widely used as a binder in the porous asphalt mix across the Netherlands. The specifications and the measured physical properties of the virgin bitumen are shown in Table 2.

Fig. 3 shows the image of the three different rejuvenators, the rejuvenator R20 and rejuvenator B are shown as a black liquid, and the

reseed oil presents in a transparent light-yellow liquid. Rejuvenator R20 and rejuvenator B used in this study were provided by Latexfalt B. V., Koudekerk aan den Rijn, the Netherlands. The rejuvenator R20 is an industrial rejuvenator which was designed to introduce the polar functionalities in asphaltene rich domains in an aged multi-phase bitumen system. According to specifications from the producer (Latexfalt), the rejuvenator R20 is especially suited for high RAP asphalt mixes produced at regular asphalt production temperature (160 °C).

Rejuvenator B is a low viscous liquid rejuvenator, which contains selected components for the re-compatibilization of the various phases in oxidized mastic, also is in particular suited for aged polymer modified asphalt and cold rejuvenation.

The rapeseed oil was purchased from De Smaakspecialist, Ulvenhout, the Netherlands. The major component of the rapeseed oil

Table 2
Physical properties of the 70/100 bitumen.

Property	Unit	Specification	Measured	Standard
Penetration at 25 °C	0.1 mm	70–100	73	EN 1426
Softening Point	°C	43–51	48	EN 1427

is unsaturated fat, which includes 27.5% polyunsaturated fat and 65% monounsaturated fat. The measured densities of rejuvenator R20, rejuvenator B and rapeseed Oil are 0.96, 0.93 and 0.90 (g/cm^3) respectively. Further in the text, the three types of rejuvenator, including rejuvenator R20, rejuvenator B and rapeseed oil, are referred as to R, B and O.

2.2. Rejuvenator evaluations

2.2.1. Bitumen ageing and rejuvenation tests

Following the European standard EN 12607–1, the Rolling Thin-Film Oven (RTFO) was employed to simulate the ageing of bitumen during its production process which refers to the short-term ageing process (STA). In the STA test, the virgin bitumen samples were kept in the cylindrical glass bottles designed for RTFO, and the test was conducted for 75 min with the oven temperature maintained at 163 °C.

Following the European standard EN 14769, the Pressure Ageing Vessel (PAV) was employed to simulate the ageing of bitumen after 5 to 10 years in service, which refers to the long-term ageing process (LTA). In the LTA test, the aged bitumen sample from RTFO test was kept a thin oven pan and then heated in the PAV at 100 °C under a pressure of 2.1 MPa for 20 h.

Rejuvenation of long-term aged bitumen is achieved by blending the aged bitumen with rejuvenator, and the rejuvenating procedure is illustrated in Fig. 4. To this aim, the aged bitumen sample was weighed and contained in an aluminium plate. Then, based on the objective dosage (1% ~ 5% by volume of bitumen where the density of the aged bitumen is 1.04 g/cm^3), the rejuvenator was carefully dropped on the bitumen sample and wetted the surface. Finally, the rejuvenated bitumen was prepared by blending the bitumen and rejuvenator under 140 °C for 20 min at 300 rpm.

2.2.2. Physical property tests

The physical properties of the bitumen sample were investigated using Needle Penetration test (NP), Ring and Ball (R&B) and Dynamic Viscosity test (DV). The NP and R&B tests were performed following the European standard EN 1426 and EN 1427, respectively. The DV tests were performed with a HAAKE RheoStress 1 viscometer, and the viscosity of a bitumen sample was measured every 10 °C from 80 to 160 °C, following EN 13302.

2.2.3. Rheological property tests

Following the European standard EN 14770, the rheological response of the bitumen samples was investigated with a frequency sweep test using a Dynamic Shear Rheometer (DSR) MCR 502 from Anton Paar, Graz, Austria (Fig. 5).

The frequency sweep tests were carried out at five different temperatures: 0, 10, 20, 30 and 40 °C, using a range of loading frequency from (0.01 Hz to 50 Hz). The tests were performed with 8 mm parallel plates, and the bitumen sample has a thickness of 2 mm. Based on the time-temperature superposition principle, the master curves of complex

modulus (G^*) and phase angle (δ) at the reference temperature (20 °C) can be obtained, by shifting with Williams–Landel–Ferry equation (1), fitting with Symmetrical Sigmoidal equation (2) and error minimizing with equation (3).

$$\log \alpha_T(T) = \frac{-C_1(T-T_0)}{[C_2 + (T-T_0)]} \tag{1}$$

Where:
α_T: is the superposition parameter;
T: is the temperature (°C);
T_0: is the reference temperature (°C);
C_1, C_2: are empirical constants;

$$\log |G^*|_{fit} = \log |G^*|_{min} + \frac{\log |G^*|_{max} - \log |G^*|_{min}}{1 + e^{\beta+\gamma(\log f + \log \alpha_T)}} \tag{2}$$

Where:
G^*: is the tested complex modulus (Pa);
f: is the loading frequency (Hz);
β, γ: are the shifting parameters;
α_T: is the shift factor;
$|G^*|_{max}$: s the assumed maximum complex modulus (Pa);
$|G^*|_{min}$: is the assumed minimum complex modulus (Pa);
$|G^*|_{fit}$: is the fitted complex modulus (Pa);

$$\sum_{n=1}^N error = \sum_{n=1}^\infty \left(\frac{\log |G^*|_{test} - \log |G^*|_{fit}}{\log |G^*|_{test}} \right)^2 \tag{3}$$

Where:
$|G^*|_{test}$: is the tested complex modulus (Pa);
$|G^*|_{fit}$: is the fitted complex modulus (Pa);
error: is the fitting error.

The rutting parameter ($G^*/\sin \delta$) and fatigue parameter ($G^* \cdot \sin \delta$) were deduced from the master curve at 10 rad/s, in which the rutting parameter reflects the irrecoverable deformation of bitumen, and the fatigue parameter represents the loss modulus of the bitumen, therefore they were used to evaluate the rutting resistance and fatigue resistance of the bitumen samples. Besides, the cracking resistance of the bitumen sample was characterized using the black space diagram. In this study, the black space diagram was divided into different crack-sensitive zones based on Glover-Rowe (G-R) parameters (4) and R-values (5), and the results from master curves were plotted at the frequency of 0.005 rad/s, 15 °C [32].

$$GR = \frac{G^* \cdot \cos^2\delta}{\sin \delta} \tag{4}$$

Where:
GR: is the G-R parameter, which is 180 kPa and 450 kPa in this study;
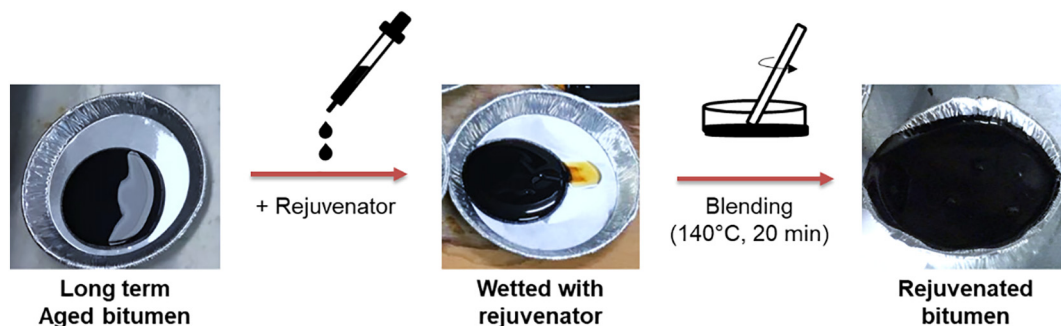G^*: is the complex modulus (kPa);
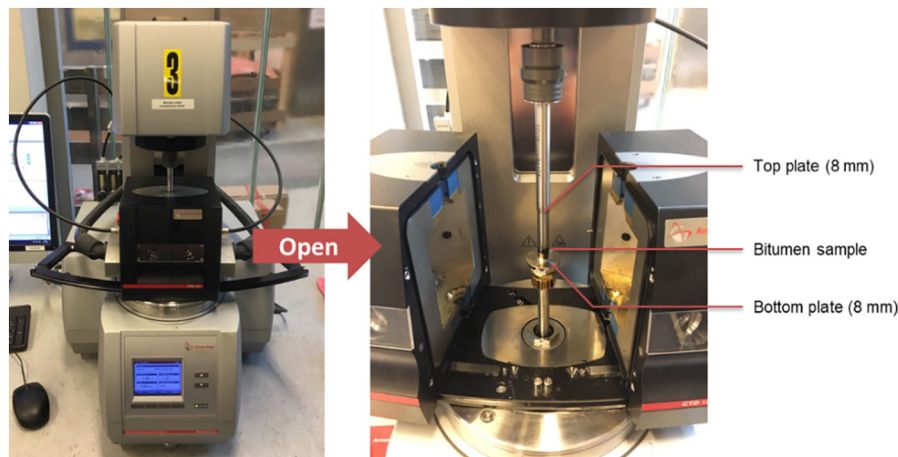

Fig. 4. The procedure of aged bitumen rejuvenation.

Fig. 5. The Dynamic Shear Rheometer MCR 502 and the bitumen sample sandwiched between 8 mm parallel plates.

δ: is the phase angle (°).

$$R = \frac{(\log 2) \cdot \log \frac{G}{G_g}}{\log \left(1 - \frac{\delta}{90}\right)} \tag{5}$$

Where:

R: is the R-value, which is 1, 2, and 3 in this study;
G^*: is the complex modulus (kPa);
G_g: is the glassy modulus, assumed to be 10^9 (Pa);
δ: is the phase angle (°).

2.2.4. Chemical property tests

Fourier-transform infrared spectroscopy (FTIR) was employed in order to study the change in bitumen chemical composition caused by the bitumen ageing [33]. The FTIR test was performed using the Spectrum 100 FT-IR spectrometer with Attenuated Total Reflectance (ATR) from PerkinElmer, United States, and each bitumen sample was scanned 20 times, at the wavenumbers from 600 to 4000 cm^{-1} with a resolution of 2 cm^{-1}.

After ageing, the infrared spectra of bitumen may show changes in peak areas at 1030 cm^{-1} and 1700 cm^{-1}, which is due to the accumulation of oxidation products during the ageing process, namely carbonyls and sulfoxides [34]. For this reason, the carbonyl index (I_c), the sulfoxide index (I_s) and the combined index ($I_c + I_s$) are usually used to quantify the ageing level in a bitumen [35], which can be calculated based on the reference area ($\sum A$) with the following equations:

$$I_c = \frac{A_{1700}}{\sum A} \tag{6}$$

$$I_s = \frac{A_{1030}}{\sum A} \tag{7}$$

$$\sum A = A_{(2953,2862)} + A_{1700} + A_{1600} + A_{1460} + A_{1376} + A_{1030} \\ + A_{864} + A_{814} + A_{743} + A_{724} \# \tag{8}$$

Following the experience of Lamontagne et al. [33], Zaumanis et al. [36] and Jing [37], the reference area ($\sum A$) used in this study is derived based on the bitumen characteristics and presented as the highlighted area in Fig. 6. Each highlighted area represents the band of a specific functional group of the bitumen, in which the carbonyl band (A1700) is selected between 1670 cm^{-1} and 1722 cm^{-1}, to exclude the characteristic peak of the rejuvenator (1743 cm^{-1}) [36]. Besides, the sulfoxide band is selected between 995 cm^{-1} and 1047 cm^{-1}.
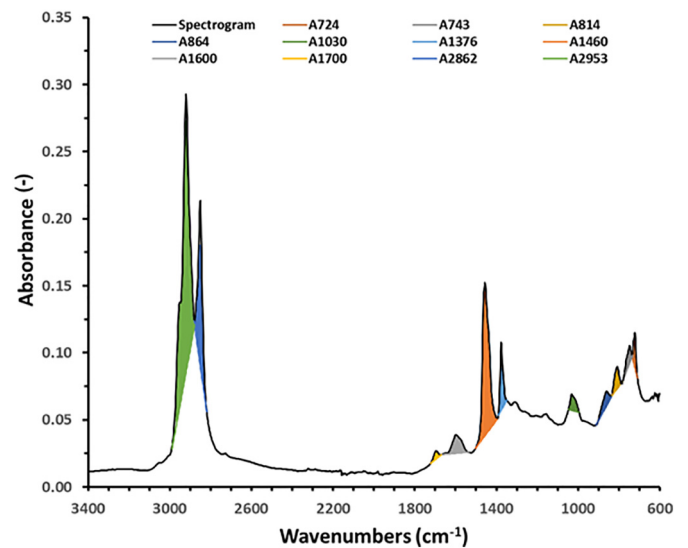

Fig. 6. The reference areas of FTIR spectrogram.

2.3. Capsule evaluations

2.3.1. Rejuvenator encapsulation procedure

Fig. 7 illustrates the rejuvenator encapsulating procedure for calcium alginate capsules, which includes three steps [38,39]:

i. **Mixing of the alginate solution with rejuvenator and PEMA.**
Two solutions, including a 6 wt% sodium alginate solution and a rejuvenator & Poly(ethylene-*alt*-maleic-anhydride) (PEMA) solution (with the ratio of 40% PEMA and 60% rejuvenator), were prepared and mixed by the alginate/rejuvenator ration of 30/70 for 30 s at 100 rpm.

ii. **Pumping and dropping into the CaCl$_2$ solution.**
The alginate and rejuvenator blend was placed in a vacuum chamber for 30 min to remove air bubbles. Then, the blend was pumped through a needle and the capsule beads were dropped into the CaCl$_2$ solution.

iii. **Capsule collecting and drying**
The capsules solidified in the CaCl$_2$ solution were collected, and the final calcium alginate capsules were acquired after drying in an oven at 30 °C for 48 h.
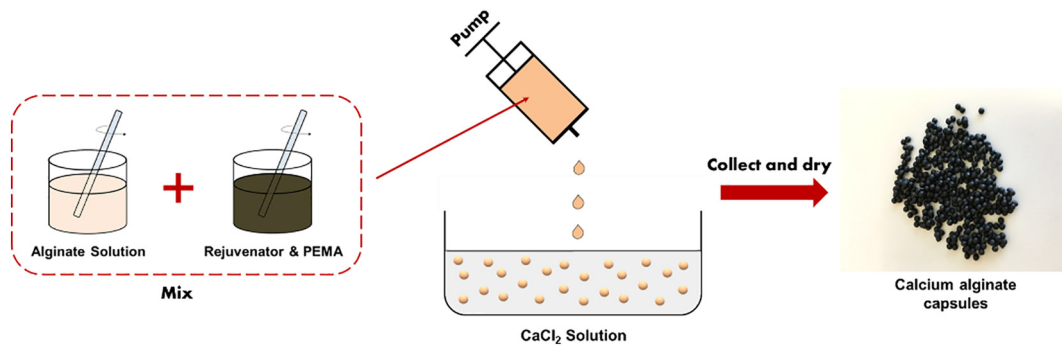
Fig. 7. Schematic of the rejuvenator encapsulation in calcium alginate capsules.

2.3.2. Capsule property tests

Light Microscopy (LM), Thermogravimetric Analysis (TGA) and Micro-compressive test (MC) were employed to evaluate the performance of calcium alginate capsules encapsulating different rejuvenators. A Leica MZ 6 light microscope device was used to observe the morphology of calcium alginate capsules. The colour and diameter of calcium alginate capsules were studied using this device.

A NETZSCH STA 449 F3 Jupiter TGA system was used to evaluate the thermal stability of calcium alginate capsules. The analysis was conducted in the environment of argon gas (Ar). A Sample Temperature Control (STC) programme was employed: the TGA test started at 40 °C and increased at the rate of 5 °C/min until 160 °C which simulated the temperature for asphalt mixing and production, then hold on 160 °C for 10 min.

A micro strength testing machine (Fig. 8) was used to investigate the mechanical response of the capsules. Fig. 8(a) shows the MC test setup where the compressive loading is applied at a displacement control of 0.01 mm/s. The tests were performed under the ambient temperature of 20 °C and a camera was used to film the testing period with which the capsule contact area can be acquired from the image process.

Fig. 8(b) shows the schematic of load vs displacement curve measured from the MC test, and the four data points in this curve can be related to different compressive stages of a capsule recorded by the camera: (1) loading start, (2) elastic response region, (3) capsule

broken and (4) end of the test. The rupture strength of a capsule is defined with the tensile hoop stress calculated at data point (3) with the following equation [40]:

$$\sigma_r = 0.4\frac{P_t}{A_t} \tag{9}$$

Where:
σ_r: is the rupture strength (MPa);
P_t: is the load at time t (N);
A_t: is the capsule cross-sectional area, at time t (m²);

3. Results and discussions

3.1. Physical properties

3.1.1. Physical properties of the aged bitumen

For the engineering purpose, bitumen is graded based on its penetration level which is described in European standard EN 12591. Table 3 summarises the bitumen specifications for grades from 20 (0.1 mm) to 100 (0.1 mm) penetration. In general, ageing leads to a change in bitumen physical properties, e.g., penetration, softening point and viscosity, which results in a decreased grade level, thus the ageing level can be evaluated by referring the bitumen grade to its original (virgin) state.
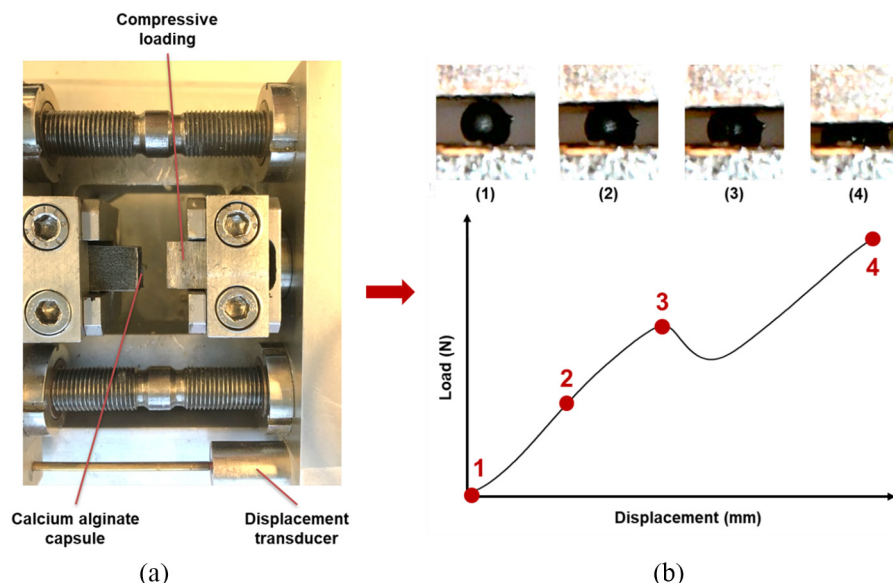

(a) (b)

Fig. 8. The micro-compressive test on a calcium alginate capsule: (a) test setup and (b) the load-displacement curve and the test images recorded from the camera.

Property	Unit	20/30	30/45	35/50	40/60	50/70	70/100
Penetration at 25 °C	0.1 mm	20–30	30–45	35–50	40–60	50–70	70–100
Softening Point	°C	55–63	52–60	50–58	48–56	46–54	43–51

The physical properties of the virgin bitumen and the results after the short-term and long-term ageing process are presented in Fig. 9. Fig. 9(a) shows that, after the short-term ageing (STA) process, the penetration and softening point of the PEN 70/100 bitumen were changed from 73 (0.1 mm) and 48 °C to 51 (0.1 mm) and 55 °C, which indicates a change of bitumen grade to 40/60. While the penetration and softening point of the long-term aged bitumen (LTA) reached 24 and 62, which refers to the PEN 20/30 bitumen. Fig. 9(b) shows that the viscosity of the bitumen is increased after ageing, and the bitumen viscosity after LTA is higher than that after STA.

A capsule healing system aims to improve the intrinsic healing capacity of the aged bitumen without causing premature damages, and as such, the released rejuvenator from capsules should not over-rejuvenating the bitumen to a grade lower than its grade after paving. Hence, the STA bitumen grade (40/60) was set as the limit of the rejuvenated bitumen, which was applied in the rejuvenator dosage determination for a capsule healing system.

3.1.2. Physical properties of the rejuvenated bitumen

Fig. 10 shows the penetration, softening point and dynamic viscosity of the long-term aged bitumen rejuvenated with R, B and O (refers to LA_R, LA_B and LA_O), with dosages from 1% to 5% (by volume of bitumen). It is found that rejuvenation of an aged bitumen leads to an increase in penetration (Fig. 10(a)) and a decrease in softening point (Fig. 10(b)), and this change becomes more significant when a higher dosage of rejuvenator is applied. Among the three types of rejuvenator, O shows the greatest changes in both penetration and softening point, which indicates the highest rejuvenation efficiency, then followed by B and R. Fig. 10(c) presents the dynamic viscosity test result which shows that, when LTA is rejuvenated with 5% of R, B and O (refers to LA_R5, LA_B5 and LA_O5), the dynamic viscosity decreases from LA_R5, LA_B5 to LA_O5 which agrees with the findings from NP and R&B.

Based on the NP and R&B results, the optimum amount of R, B and O can be determined for the application in capsule healing system. The dash-lines in Fig. 10(a) and (b) indicate the values for PEN 40/60 bitumen which refers to the objective grade for the rejuvenated bitumen. When the penetration values reach 40 (0.1 mm), the optimum amount of R, B and O are determined following the trend of penetration values with rejuvenator dosages, which are 3.9%, 2.7% and 2.2%, respectively. However, the softening point of the aged bitumen blended with 3.9% R is beyond the upper limit of PEN 40/60. Although it does not fulfil the requirement of PEN 40/60, it is more stable with better resistance to the temperature changes.

3.2. Rheological properties

3.2.1. Complex modulus and phase angle

Fig. 11 shows the master curves of complex modulus and phase angle of the 70/100 bitumen at different ageing levels. Compared to the virgin 70/100 bitumen, STA showed higher complex modulus and lower phase angle, while the LTA showed more significant changes in complex modulus and phase angle.

Fig. 12 shows the master curves of the bitumen samples, namely LA_R3, LA_B3 and LA_O3 (with 3% R, B and O, respectively), and their status after re-ageing, namely RA_R3, RA_B3 and RA_O3. The complex modulus and phase angle of LTA is also plotted as a reference. The complex modulus of LA_R3 is much higher than LA_O3, which indicates that the complex modulus of the aged bitumen can be reduced more significantly when blended with O than R. The complex modulus master curve of LA_B3 generally locates between the curves of LA_R3 and LA_O3, which overlaps with LA_R3 in the low-frequency region and LA_O3 in high-frequency region, therefore B has an intermediate complex modulus reducing effect, which also indicates that LA_B3 has the best low temperature and high temperature performance. The phase angle of the rejuvenated bitumen samples decreases from LA_R3, LA_B3 to LA_O3, which indicates that the rejuvenator's ability to restore the phase angle decreases from R, B and O.

The rejuvenated bitumen becomes brittle after the re-ageing process, which can be observed in Fig. 12 where the complex modulus grows higher and the phase angle becomes lower. The LTA samples rejuvenated with B and O all showed significant changes in both complex modulus and phase angle, and their changing amplitude is much greater than those rejuvenated with R. Hence, aged bitumen rejuvenated with R
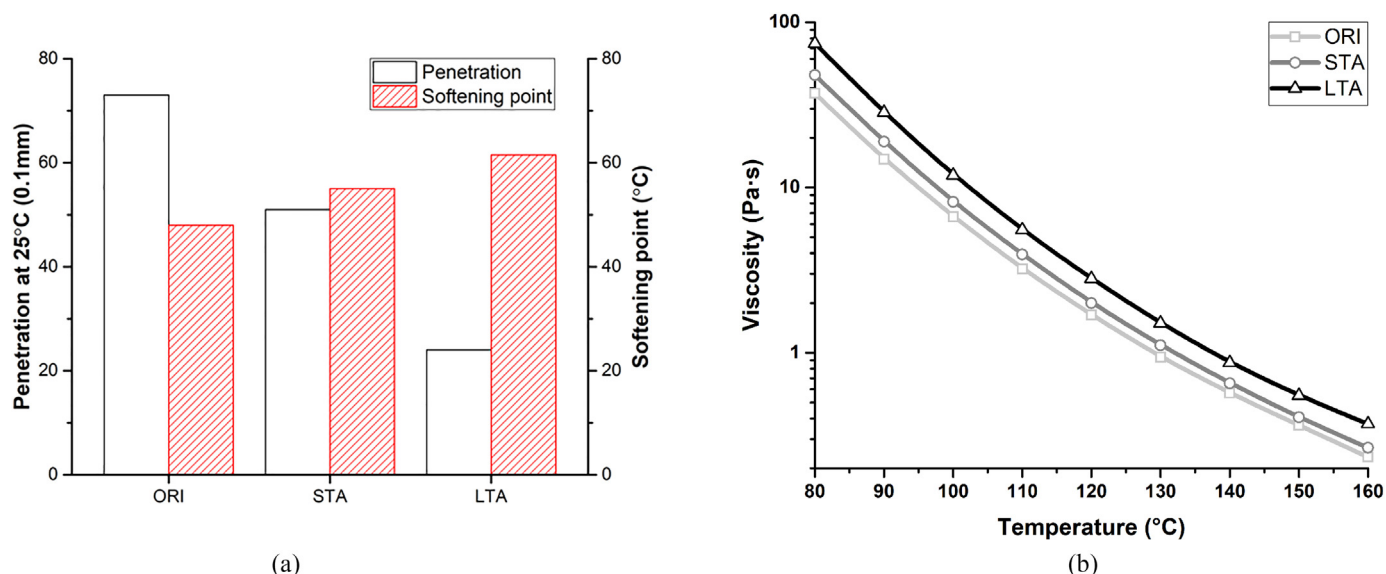

(a)

(b)

Fig. 9. Physical properties of the 70/100 bitumen at different ageing levels: (a) Penetration and softening point and (b) dynamic viscosity.
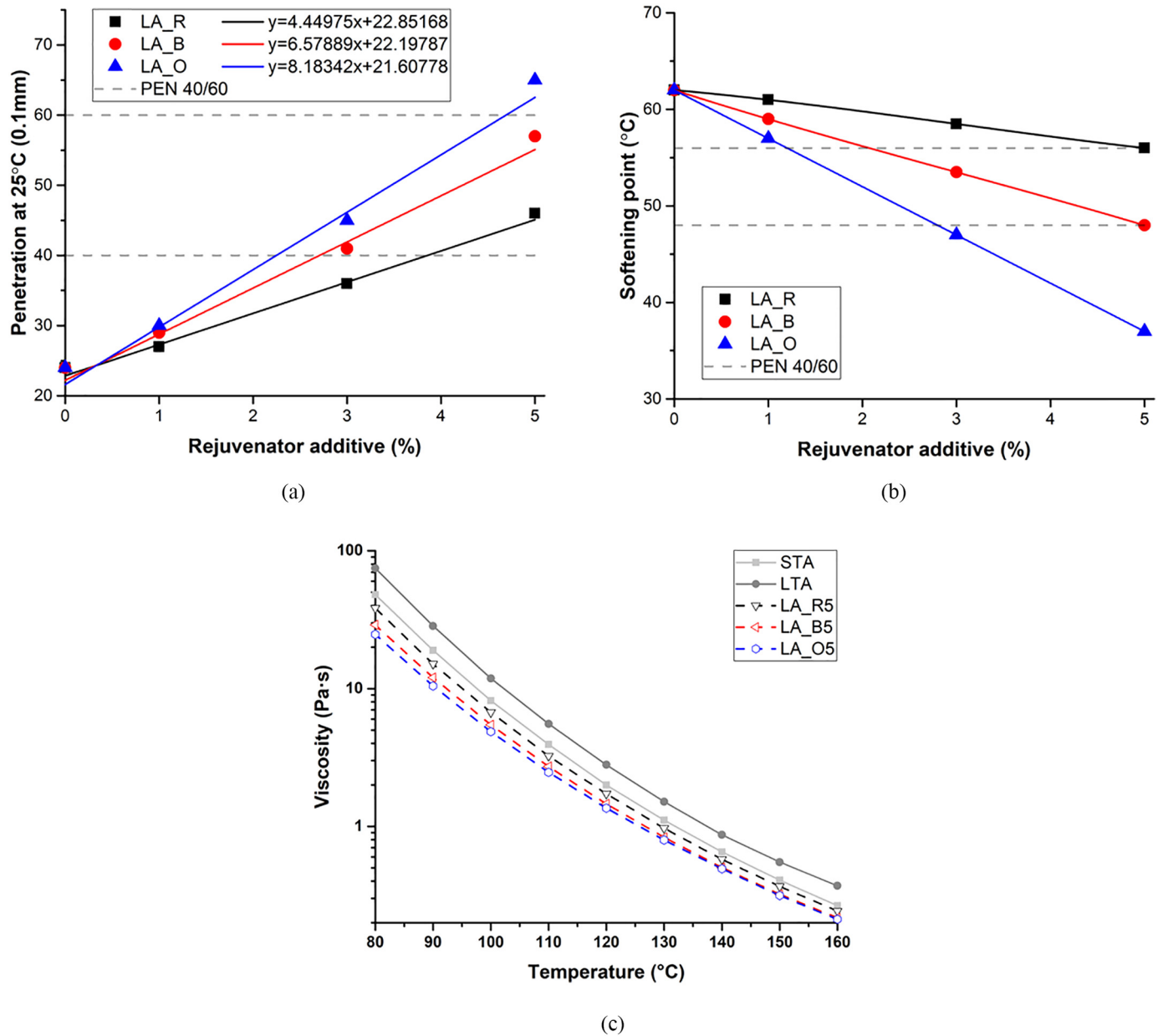
(a)

(b)

(c)

Fig. 10. The physical properties of the rejuvenated bitumen: (a) penetration, (b) softening point and (c) dynamic viscosity.

will demonstrate a more stable behaviour in time and the material is less prone to ageing than the other re-aged rejuvenated samples.

3.2.2. Rutting and fatigue resistance

Fig. 13 shows the rutting parameter and fatigue parameter of the rejuvenated bitumen samples at 20 °C and their status after re-ageing, and the results of STA are plotted with dash-lines as references. As shown in Fig. 13(a), for the rejuvenated bitumen, the bitumen sample blended with 3% R showed a higher rutting parameter thus a better rutting resistance which might be due to LA_R3 had the highest complex modulus (see Fig. 12). After re-ageing, all these rejuvenated bitumen samples showed improved rutting resistances, and RA_O3 became even higher than RA_R3 as a result of significantly increased modulus for O rejuvenated bitumen.

Fig. 13(b) shows that the fatigue parameter for LA_R3 is much higher than LA_B3 and LA_O3, which indicates a lower fatigue resistance. However, the difference of fatigue parameters for three different bitumen

samples becomes much lower after re-ageing, which indicates the fatigue resistance of the R rejuvenated bitumen decreases much slower in the ageing process. Besides, the fatigue parameters for all the bitumen samples are below 5 MPa which satisfies the limit of PAV aged bitumen determined in SHRP.

3.2.3. Black space diagram

In the black space diagram, a range of G-R values between 180 kPa and 450 kPa can be used to predict the onset and propagation of damage which refers to the damage zone, and the area below is regarded as no block cracking zone [32,41]. R-values can further divide the black space diagram into different crack-sensitive regions where a higher R-value indicates the greater cracking potential [32].

Fig. 14 shows the black space diagram of the bitumen samples based on the cracking prediction with G-R parameters and R-values. In general, ageing made the bitumen brittle, which results in a change in black space diagram that drives the data of a bitumen sample moves
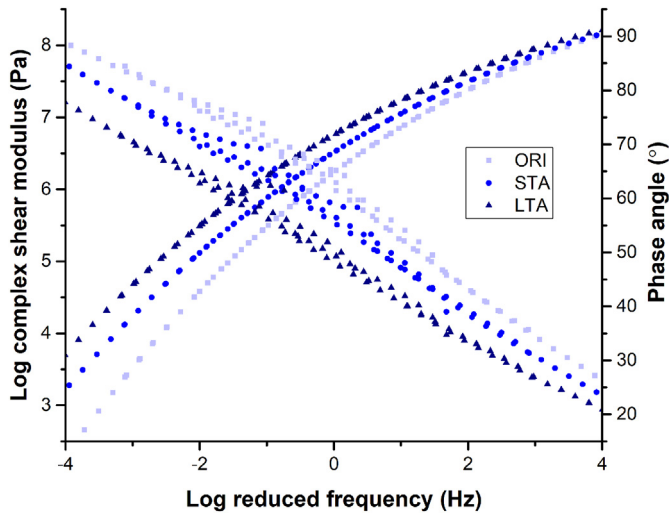
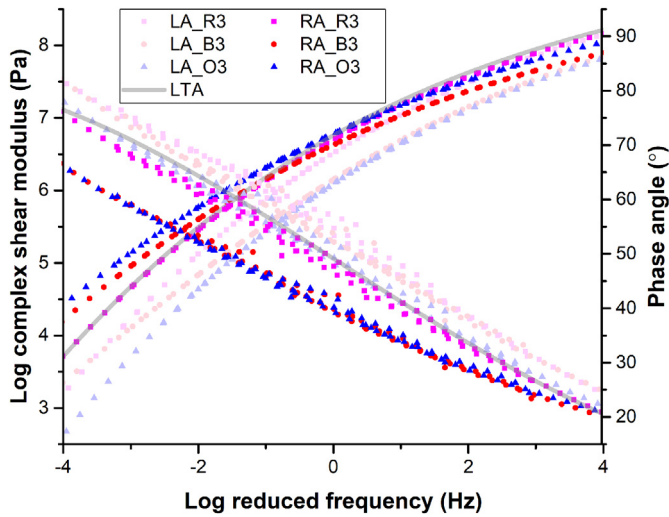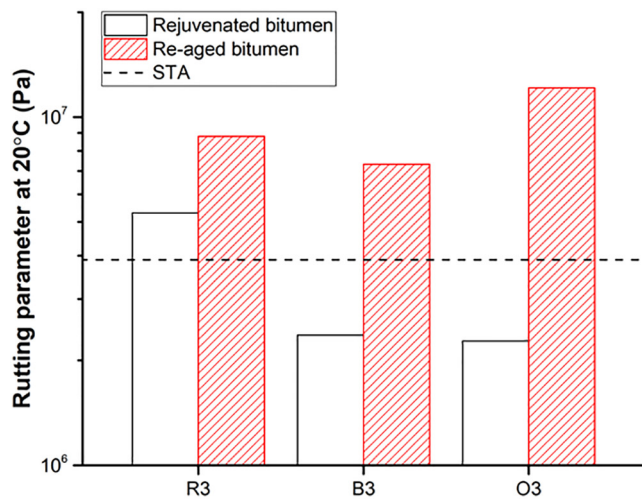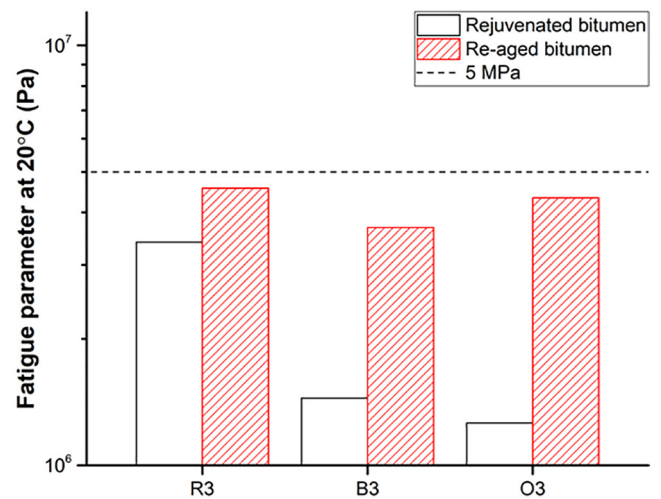Fig. 11. Master curves of the 70/100 bitumen at different ageing levels.

Fig. 14. The black space diagram at 15 °C and 0.005 rad/s divided with R-values.

Fig. 12. Master curves of the rejuvenated bitumen samples and their status after re-ageing.

to the upper left, therefore a higher cracking potential, and this can be found in the development from ORI to LTA. All the tested bitumen samples are located below the damage zone within the region between $R = 1$ and $R = 3$, which indicates no significant block cracking is expected for these bitumen samples. However, LA_R3 is in the region between R = 1 and R = 2, as such less cracking potential than LA_B3 and LA_O3. Furthermore, the bitumen samples blended with B and O showed more significant changes after re-ageing than samples blended with R. Hence, R can better improve the cracking resistance of the aged bitumen, especially after another long-term ageing process.

3.3. Chemical properties

3.3.1. Chemical composition of the aged bitumen and different rejuvenators

Fig. 15 shows the FTIR spectrogram and the ageing indices of 70/100 bitumen at different ageing levels. Fig. 15(a) shows that increased peak area at 1030 cm^{-1} and 1700 cm^{-1} are found on STA compared to ORI, which indicates an increased number of carbonyl groups and sulfoxide

(a)

(b)

Fig. 13. The rutting parameter and fatigue parameter for the rejuvenated bitumen and re-aged bitumen.

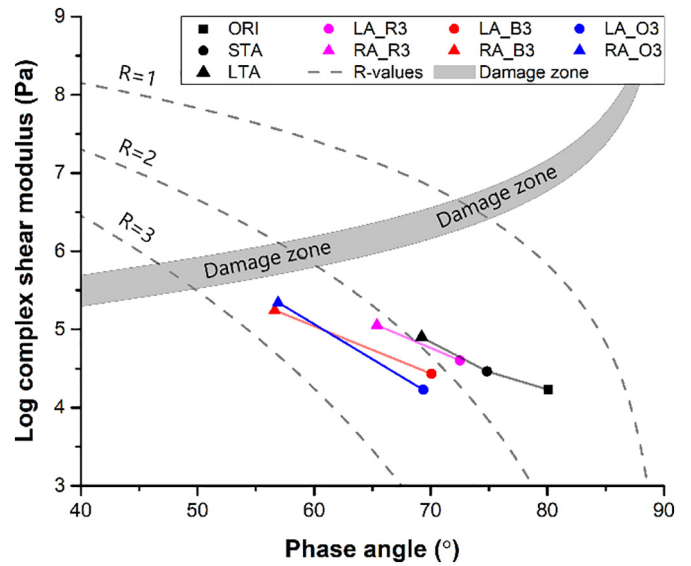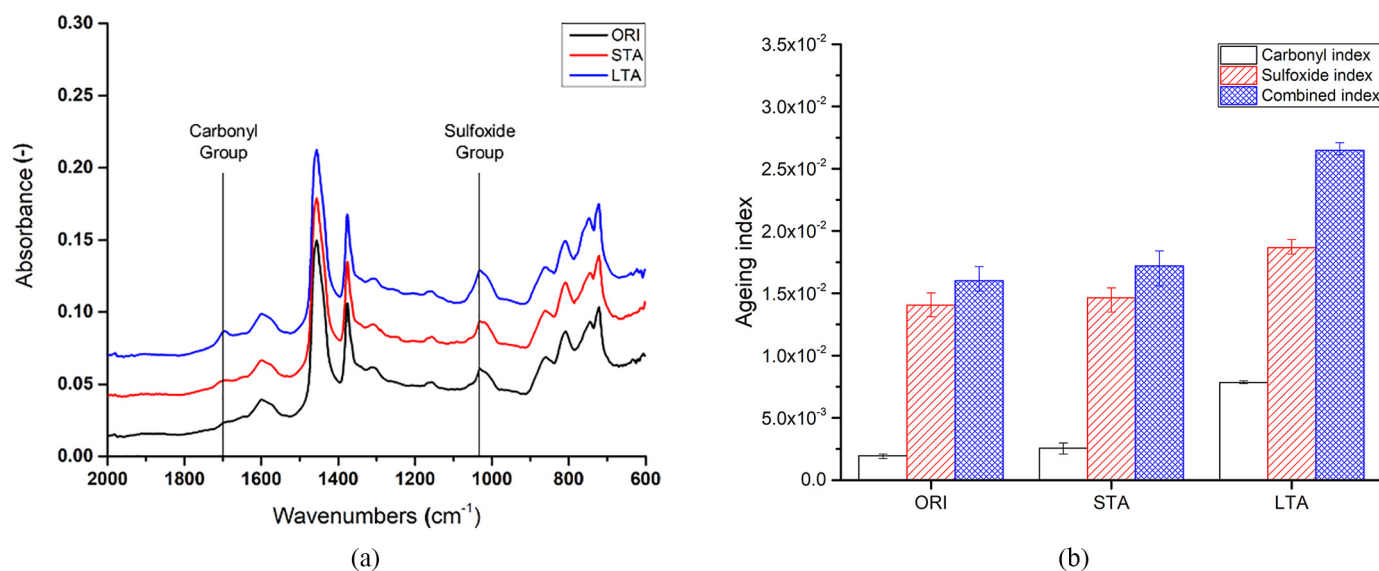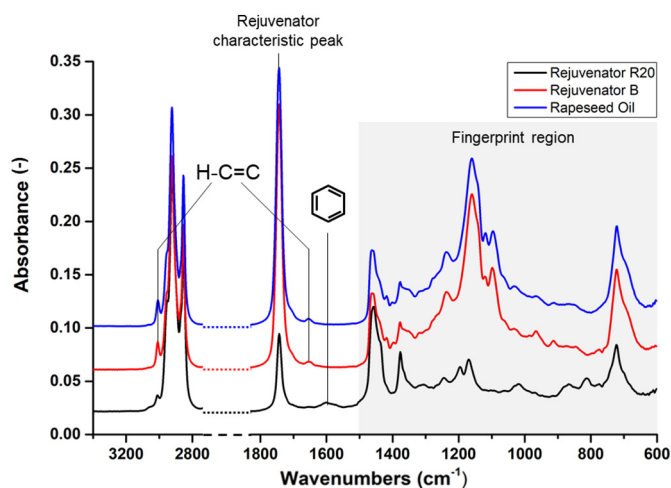Fig. 15. The FTIR results of the 70/100 bitumen at different ageing levels.

Fig. 16. The FTIR spectrogram of the three different types of rejuvenator.

groups as a result of oxidation, and the changes become more significant for LTA. Fig. 15(b) presents the ageing indices of ORI, STA and LTA.

Fig. 16 shows the chemical composition of three different types of rejuvenator characterized using FTIR. A significant absorbance peak at 1743 cm^{-1} is found in the spectra for all three types of rejuvenator which is regarded as the characteristic peak for rejuvenator. In the spectrum of rapeseed oil, the absorbance bands at 1660 cm^{-1} and 3010 cm^{-1} are due to the alkenyl C=C stretch and the relative C–H stretch from the rich unsaturated fat content [9,11]. Rejuvenator B shows a similar spectrum to rapeseed oil, and the presence of unsaturated groups can also be detected with the absorbance bands at 1660 cm^{-1} and 3010 cm^{-1}. The rejuvenator R20 shows absorbance bands at 1600 cm^{-1} which might be due to the aromatic C=C bending vibrations from the polar functionalities. Besides, these results also indicate that the chemical composition of rejuvenator R20 is very different from rejuvenator B and Oil.

3.3.2. Chemical composition of the rejuvenated bitumen

The FTIR spectrogram and the combined index of the rejuvenated and the re-aged bitumen samples are shown in Fig. 17. Fig. 17

(a) shows the FTIR spectrogram of bitumen samples rejuvenated with R, B and O 3% and their status after re-ageing. Incorporating a rejuvenator in LTA results in a growth of the absorbance bands at 1743 cm^{-1}, which is the evidence for the presence of R, B or O. Fig. 17(a) shows that LA_R3 and LA_B3 have no significant change nor development of new absorbance bands after re-ageing. However, the rejuvenator characteristic peak of LA_O3 is largely decreased after re-ageing which might be due to the emissions contained C=O (e.g., aldehydes, ketones) formed from the rapeseed oil degradation [42], thus a less fat content and weaker absorption at the characteristic peak of O (1743 cm^{-1}). Fig. 17(b) shows the combined healing index of the rejuvenated and the re-aged bitumen which indicates that, although LA_R3 shows the highest ageing index, it becomes the lowest after re-ageing, thus a more stable behaviour than LA_B3 and LA_O3.

3.4. Characterization of capsules with different rejuvenators

3.4.1. Optical microscopy

Following the rejuvenator encapsulation procedure described in 2.2.1, the calcium alginate capsules encapsulating different rejuvenators were prepared. Fig. 18 presents the optical microscopic images of the calcium alginate capsules. These capsules are presented in different colours which are determined by the encapsulated rejuvenator. The capsule encapsulating R (Cap_R) has the largest diameter of 1.95 mm, while the diameters for capsule encapsulating B (Cap_B) and O (Cap_O) are 1.44 mm and 1.38 mm, respectively. The difference in capsule diameter might be because of the different densities of these rejuvenators which resulted in different morphologies of the capsule beads formed during the dropping process of capsule preparation procedure (step ii).

3.4.2. Thermal stability

Fig. 19 shows the TGA results of calcium alginate capsules encapsulating different rejuvenators. Following the STC programme, all three types of capsules showed a stable behaviour below 100 °C and the mass loss was within 2%. Afterwards, the mass loss of these capsules grew with the temperature increasing with might be due to the weight loss from calcium alginate [39], and Cap_R showed optimal thermal stability which had the lowest mass loss, while the highest mass loss was found in Cap_O. The general trend of the thermal stability of these capsules characterized by the TGA tests agrees with the rejuvenator stability evaluated from the re-aged rejuvenator-bitumen blends, which
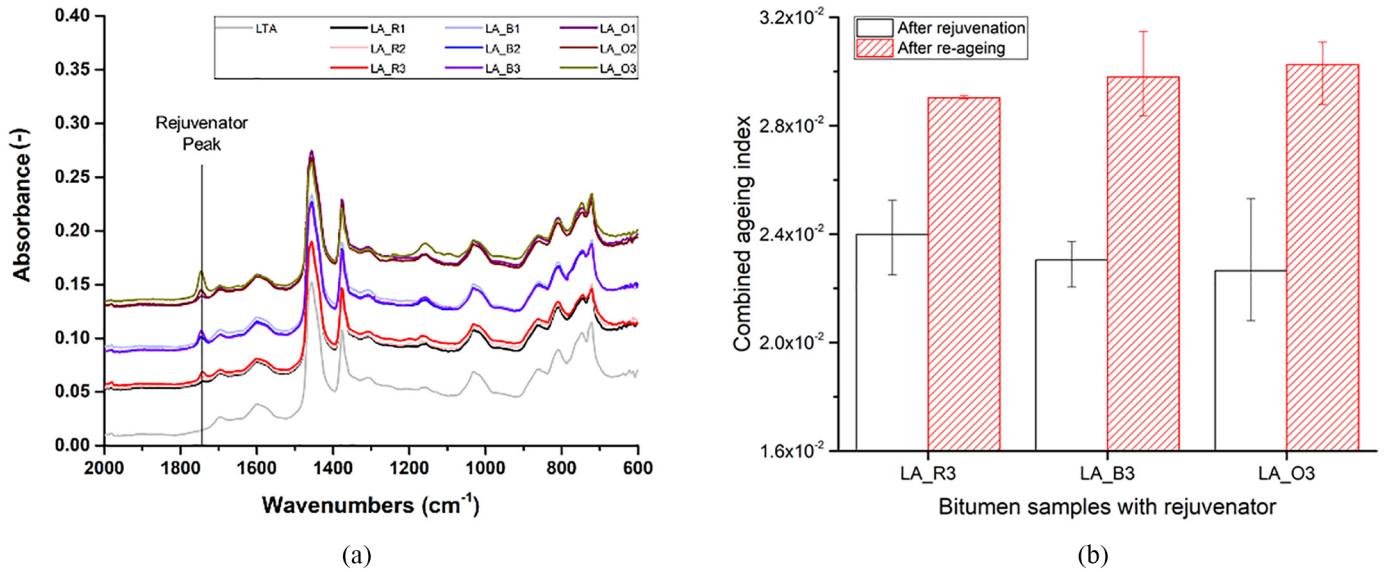
(a)

(b)

Fig. 17. The FTIR results of the rejuvenated and the re-aged bitumen samples: (a) the spectrogram of the rejuvenated and the re-aged bitumen samples, and (b) their combined index.

means the stability of the encapsulated rejuvenator might affect the thermal stability of the capsule. It is also noticed that due to the en-capsulated rejuvenators, the capsules show different diameters as such various relative surface area, which means the Cap_O that has the largest relative surface area is easier to dehydrate during the heating process.

3.4.3. Mechanical response

Fig. 20 shows the rupture strength of calcium alginate capsules en-capsulating different rejuvenators. The average rupture strength of Cap_R, Cap_B and Cap_O is 2.9, 10.3 and 10.5 MPa, respectively, and all these values are much higher than the pressure from vehicle load-ings [43] which indicates that, if these capsules survive the asphalt mixing and production process, they are able to show elastic behav-iour upon the dynamic vehicle loadings until the capsules get dam-aged from the accumulation of fatigue damage or from crack penetrating. The compressive test results also indicate that the me-chanical response of the calcium alginate capsules is largely deter-mined by the encapsulated rejuvenator. It is also noticed that smaller capsules showed a higher rupture strength, which might be related to the size effect.
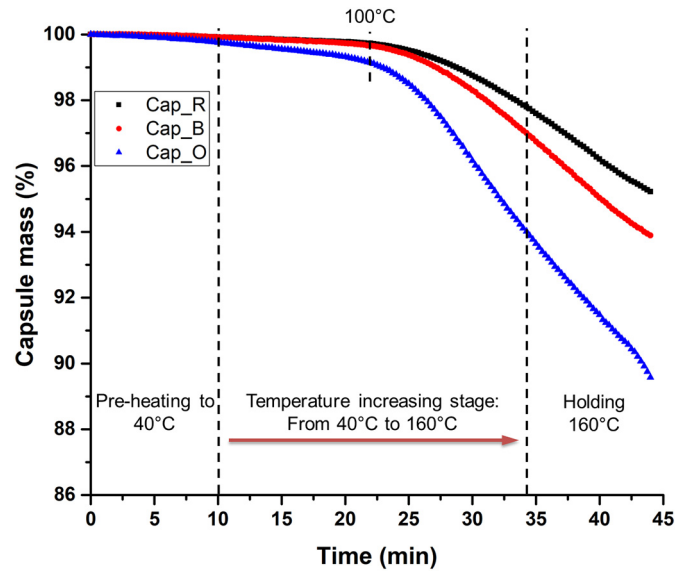
Fig. 19. The TGA results of calcium alginate capsules encapsulating different rejuvenators.

Cap_R (1.95 mm)
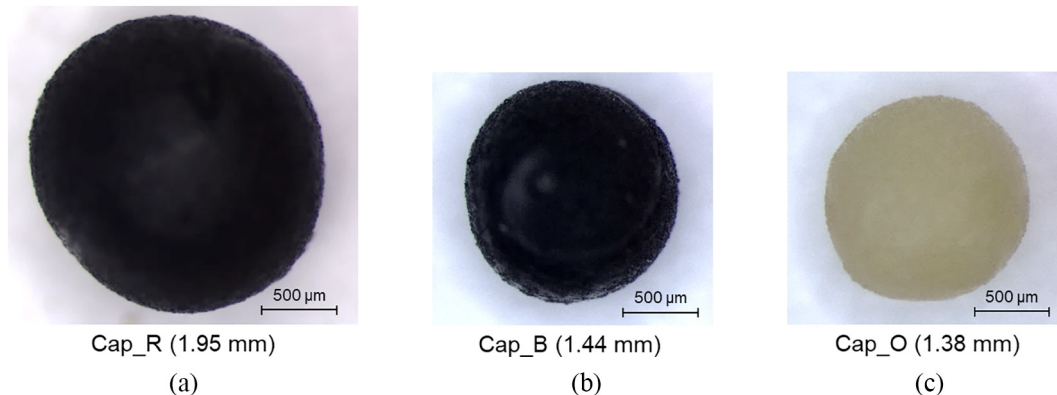
(a)

Cap_B (1.44 mm)

(b)

Cap_O (1.38 mm)

(c)

Fig. 18. The optical microscopic images of the calcium alginate capsules: (a) capsule encapsulating R, (b) capsule encapsulating B and (c) capsule encapsulating O.
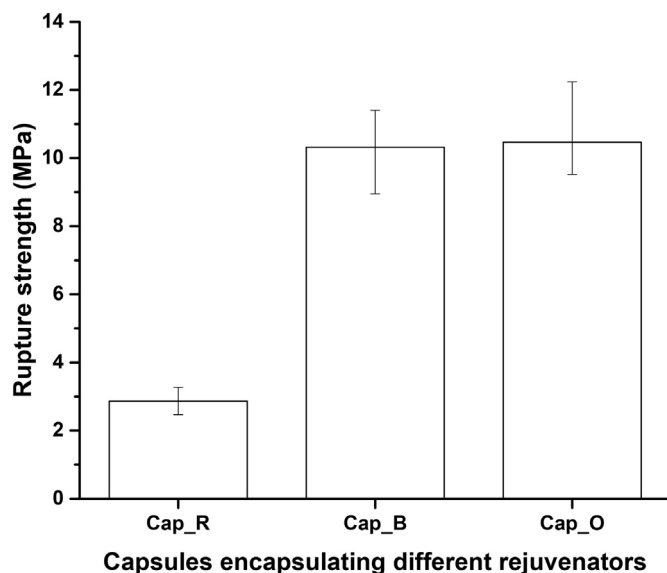
Fig. 20. The rupture strength of calcium alginate capsules encapsulating different rejuvenators.

4. Conclusions

The main objective of this study is to clarify the important role of bitumen rejuvenator for the embedded damage healing in asphalt pavement. To this aim, three different bitumen rejuvenators were evaluated based on the performance of the rejuvenated bitumen and the prospect for being encapsulated in the calcium alginate capsules. The following conclusions can be drawn:

- All three types of tested rejuvenator, namely rejuvenator R20, rejuvenator B and rapeseed Oil (R, B and O) are able to restore the physical properties of the aged bitumen, namely improve the penetration and reduce the softening point and viscosity. However, their efficiency to restore the bitumen physical properties decreases from O, B to R. A similar trend is also found in complex modulus. Based on the penetration values, the recommended dosages for R, B and O are obtained, which are 3.9%, 2.7% and 2.2%, respectively.
- The three types of rejuvenator show different capacity to restore the phase angle of the LTA which decreases from R, B to O. Besides, based on the results from rutting parameter and black space diagram, the rutting and cracking resistance of different types of rejuvenator decreases from R, B to O. Although LA_R shows lower fatigue resistance, its fatigue resistance is more stable during the ageing process than LA_B and LA_O.
- The DSR and FTIR results on re-aged bitumen indicate that the bitumen samples rejuvenated with R showed less changes in both rheological properties and chemical properties than those with B and O, thus a more stable behaviour in the long-term service.
- The encapsulated rejuvenator largely determines the performance of the calcium alginate capsules. Among the three types of calcium alginate capsules, Cap_R has the largest diameter, highest thermal stability and lowest rupture strength, Cap_O has the smallest diameter, lowest thermal stability and highest rupture strength and the performance of Cap_B are between Cap_R and Cap_O.

Based on these findings, O is determined as the most efficient rejuvenator which can soften the aged bitumen to a required level with the least amount of rejuvenator. R is determined as the best performing rejuvenator since its rejuvenated bitumen showed the best rutting and cracking resistance, and the restored properties are more stable in the next ageing period. Compared with O and R, B showed an intermediate

rejuvenation efficiency and a relatively better performance under low temperature and high temperature. Nevertheless, the life extension prospect of an asphalt pavement with capsule healing system is largely determined by the durability of the rejuvenated asphalt binder. As such, based on the evaluations of the rejuvenated bitumen, R is determined as the most suitable type of rejuvenator for the capsule healing system and the recommended amount is 3.9% (by volume of bitumen).

5. Recommendations

The type of rejuvenator which determines the capsule performance is recommended to be considered in the optimization of an encapsulation technique. In general, capsules with a smaller diameter may have better distribution in asphalt mix, while a higher capsule thermal and mechanical resistance may contribute to a better chance to survive the asphalt mixing and production process. However, if capsules are too strong, they may have problem in rejuvenator releasing when healing is needed, as such the encapsulated rejuvenator (capsule) needs to be further evaluated in an asphalt mix.

It is also noticed that the optimal rejuvenator type and amount are proposed based on the condition that rejuvenator and aged bitumen are evenly mixed. However, in the capsule healing system, the encapsulated rejuvenator is gradually released, then the released rejuvenator needs to diffuse slowly into the aged bitumen, and the rejuvenator releasing and diffusion process will become the research interest in the future.

CRediT authorship contribution statement

S. Xu: Investigation, Methodology, Data curation, Writing - original draft. **X. Liu:** Supervision, Writing - review & editing. **A. Tabaković:** Supervision, Writing - review & editing. **P. Lin:** Investigation, Writing - review & editing. **Y. Zhang:** Investigation, Writing - review & editing. **S. Nahar:** Methodology, Writing - review & editing. **B.J. Lommerts:** Resources, Writing - review & editing. **E. Schlangen:** Conceptualization, Resources, Supervision, Writing - review & editing.

Declaration of Competing Interest

None.

References

[1] H. Zhang, J. Yu, Z. Feng, L. Xue, S. Wu, Effect of aging on the morphology of bitumen by atomic force microscopy, J. Microsc. 246 (1) (2012) 11–19.
[2] R. Jing, X. Liu, A. Varveri, A. Scarpas, S. Erkens, The effect of ageing on chemical and mechanical properties of asphalt mortar, Appl. Sci. 8 (11) (2018) 2231.
[3] Y. Zhang, Z. Leng, Quantification of bituminous mortar ageing and its application in ravelling evaluation of porous asphalt wearing courses, Mater. Des. 119 (2017) 1–11.
[4] Y. Tong, R. Luo, R.L. Lytton, Moisture and aging damage evaluation of asphalt mixtures using the repeated direct tensional test method, Int. J. Pavement Eng. 16 (5) (2015) 397–410.
[5] X. Hou, F. Xiao, J. Wang, S. Amirkhanian, Identification of asphalt aging characterization by spectrophotometry technique, Fuel 226 (2018) 230–239.

[6] T. Ma, X. Huang, Y. Zhao, Y. Zhang, Evaluation of the diffusion and distribution of the rejuvenator for hot asphalt recycling, Constr. Build. Mater. 98 (2015) 530–536.

[7] D. Kuang, J. Yu, H. Chen, Z. Feng, R. Li, H. Yang, Effect of rejuvenators on performance and microstructure of aged asphalt, J. Wuhan Univ. Technol. Mater. Sci. Ed. 29 (2) (2014) 341–345.

[8] S. Nahar, Phase-Separation Characteristics of Bitumen and their Relation to Damage-Healing, Delft University of Technology, 2016.

[9] A. Behnood, Application of rejuvenators to improve the rheological and mechanical properties of asphalt binders and mixtures: a review, J. Clean. Prod. 231 (2019) 171–182.

[10] Z. Sun, J. Yi, Y. Huang, D. Feng, C. Guo, Properties of asphalt binder modified by bio-oil derived from waste cooking oil, Constr. Build. Mater. 102 (2016) 496–504.

[11] M. Chen, F. Xiao, B. Putman, B. Leng, S. Wu, High temperature properties of rejuvenating recovered binder with rejuvenator, waste cooking and cotton seed oils, Constr. Build. Mater. 59 (2014) 10–16.

[12] R. Romera, A. Santamaría, J.J. Peña, M.E. Muñoz, M. Barral, E. García, V. Jañez, Rheological aspects of the rejuvenation of aged bitumen, Rheol. Acta 45 (4) (2006) 474–478.

[13] M. Pasetto, A. Baliello, G. Giacomello, E. Pasquini, A rheological study on rejuvenated binder containing very high content of aged bitumen, RILEM 252-CMB-Symposium on Chemo Mechanical Characterization of Bituminous Materials, Springer 2018, pp. 183–188.

[14] T.B. Moghaddam, H. Baaj, The use of rejuvenating agents in production of recycled hot mix asphalt: a systematic review, Constr. Build. Mater. 114 (2016) 805–816.

[15] H.M. Silva, J.R. Oliveira, C.M. Jesus, Are totally recycled hot mix asphalts a sustainable alternative for road paving? Resour. Conserv. Recycl. 60 (2012) 38–48.

[16] J. Qiu, M. Huurman, B. de Bruin, E. Demmink, M. Frunt, Towards 90% warm re-use of porous asphalt using foaming technology, J. Clean. Prod. 190 (2018) 251–260.

[17] I.L. Al-Qadi, M. Elseifi, S.H. Carpenter, Reclaimed asphalt pavement—a literature review, The Illinois Digital Environment for Access to Learning and Scholarship, 2007.

[18] O. Reyes-Ortiz, E. Berardinelli, A.E. Alvarez, J. Carvajal-Muñoz, L. Fuentes, Evaluation of hot mix asphalt mixtures with replacement of aggregates by reclaimed asphalt pavement (RAP) material, Procedia Soc. Behav. Sci. 53 (2012) 379–388.

[19] J. Brownridge, The role of an asphalt rejuvenator in pavement preservation: use and need for asphalt rejuvenation, Compendium of Papers from the First International Conference on Pavement Preservation 2010, pp. 351–364.

[20] Á. García, E. Schlangen, M. van de Ven, G. Sierra-Beltrán, Preparation of capsules containing rejuvenators for their use in asphalt concrete, J. Hazard. Mater. 184 (1–3) (2010) 603–611.

[21] S. Xu, A. Tabaković, X. Liu, E. Schlangen, Preparation of Calcium Alginate Capsules and the Application in Asphalt Mastic, 6th International Conference on Self-Healing Materials, Friedrichshafen, Germany, 2017.

[22] S. Xu, X. Liu, A. Tabaković, E. Schlangen, A novel self-healing system: towards a sustainable porous asphalt, J. Clean. Prod. 120815 (2020).

[23] J. Norambuena-Contreras, E. Yalcin, A. Garcia, T. Al-Mansoori, M. Yilmaz, R. Hudson-Griffiths, Effect of mixing and ageing on the mechanical and self-healing properties of asphalt mixtures containing polymeric capsules, Constr. Build. Mater. 175 (2018) 254–266.

[24] T. Al-Mansoori, J. Norambuena-Contreras, R. Micaelo, A. Garcia, Self-healing of asphalt mastic by the action of polymeric capsules containing rejuvenators, Constr. Build. Mater. 161 (2018) 330–339.

[25] A. Tabaković, W. Post, D. Cantero, O. Copuroglu, S. Garcia, E. Schlangen, The reinforcement and healing of asphalt mastic mixtures by rejuvenator encapsulation in alginate compartmentalised fibres, Smart Mater. Struct. 25 (8) (2016), 084003, .

[26] B. Shu, S. Wu, L. Dong, J. Norambuena-Contreras, Y. Li, C. Li, X. Yang, Q. Liu, Q. Wang, F. Wang, Self-healing capability of asphalt mixture containing polymeric composite fibers under acid and saline-alkali water solutions, J. Clean. Prod. 122387 (2020).

[27] J.-F. Su, J. Qiu, E. Schlangen, Stability investigation of self-healing microcapsules containing rejuvenator for bitumen, Polym. Degrad. Stab. 98 (6) (2013) 1205–1215.

[28] A. Garcia, J. Jelfs, C.J. Austin, Internal asphalt mixture rejuvenation using capsules, Constr. Build. Mater. 101 (2015) 309–316.

[29] S. Shirzad, M.M. Hassan, M.A. Aguirre, L.N. Mohammad, W.H. Daly, Evaluation of sunflower oil as a rejuvenator and its microencapsulation as a healing agent, J. Mater. Civ. Eng. 28 (11, 2016), 04016116, .

[30] M. Zaumanis, R.B. Mallick, R. Frank, Evaluation of rejuvenator's effectiveness with conventional mix testing for 100% reclaimed asphalt pavement mixtures, Transp. Res. Rec. 2370 (1) (2013) 17–25.

[31] A. Ongel, M. Hugener, Impact of rejuvenators on aging properties of bitumen, Constr. Build. Mater. 94 (2015) 467–474.

[32] G. King, M. Anderson, D. Hanson, P. Blankenship, Using black space diagrams to predict age-induced cracking, 7th RILEM International Conference on Cracking in Pavements, Springer 2012, pp. 453–463.

[33] J. Lamontagne, P. Dumas, V. Mouillet, J. Kister, Comparison by Fourier transform infrared (FTIR) spectroscopy of different ageing techniques: application to road bitumens, Fuel 80 (4) (2001) 483–488.

[34] C. Xing, L. Liu, Y. Cui, D. Ding, Analysis of base bitumen chemical composition and aging behaviors via atomic force microscopy-based infrared spectroscopy, Fuel 264 (2020) 116845.

[35] X. Lu, U. Isacsson, Effect of ageing on bitumen chemistry and rheology, Constr. Build. Mater. 16 (1) (2002) 15–22.

[36] M. Zaumanis, M.C. Cavalli, L.D. Poulikakos, Comparing Different Rejuvenator Addition Locations in Asphalt Plant Based on Mechanical and Chemical Properties of Binder, Transportation Research Board 97th Annual Meeting, Washington DC, 2018.

[37] R. Jing, Ageing of Bituminous Materials: Experimental and Numerical Characterization, Delft University of Technology, 2019.

[38] S. Xu, A. Tabaković, X. Liu, D. Palin, E. Schlangen, Optimization of the calcium alginate capsules for self-healing asphalt, Appl. Sci. 9 (3) (2019) 468.

[39] S. Xu, A. Tabaković, X. Liu, E. Schlangen, Calcium alginate capsules encapsulating rejuvenator as healing system for asphalt mastic, Constr. Build. Mater. 169 (2018) 379–387.

[40] V. Pejchal, G. Zagar, R.L. Charvet, C. Dénéréaz, A. Mortensen, Compression testing spherical particles for strength: Theory of the meridian crack test and implementation for microscopic fused quartz, J. Mech. Phys. Solids 99 (2016).

[41] G. Rowe, G. King, M. Anderson, The influence of binder rheology on the cracking of asphalt mixes in airport and highway projects, J. Test. Eval. 42 (5) (2014) 1063–1072.

[42] H.R. Katragadda, A. Fullana, S. Sidhu, Á.A. Carbonell-Barrachina, Emissions of volatile aldehydes from heated cooking oils, Food Chem. 120 (1) (2010) 59–65.

[43] E.R. Brown, P.S. Kandhal, J. Zhang, Performance testing for hot mix asphalt, National Center for Asphalt Technology Report (01–05, 2001), 2001.